Two-parameter areal scaling in the Hénon map

Gonzalo Marcelo Ramírez-Ávila[1,2,3], Imre M. Jánosi[1,3,4] and Jason A.C. Gallas[1,2,3,5]

[1] Max-Planck Institute for the Physics of Complex Systems, Nöthnitzer Str. 38, 01187 Dresden, Germany,
[2] Instituto de Investigaciones Físicas, Campus Cota-Cota, Universidad Mayor de San Andrés, La Paz, Bolivia,
[3] Instituto de Altos Estudos da Paraíba, Rua Silvino Lopes 419-2502, 58039-190 João Pessoa, Brazil,
[4] Department of Physics of Complex Systems, Eötvös Loránd University, H-1117 Budapest, Hungary,
[5] Complexity Sciences Center, 9225 Collins Avenue Suite 1208, Surfside FL 33154, USA.

PACS 05.45.-1 – Nonlinear dynamics and chaos
PACS 02.70.-c – Computational techniques; simulations
PACS 02.70.Rr – General statistical methods

Abstract – We study a bifurcation cascade whose proper unfolding requires tuning more than one parameter simultaneously. Specifically, we investigate metric properties of extended self-similar triangular areas observed recently in the control parameter space of flows (lasers and electronic circuits), and maps. Such areas are delimited by shrimplike stability islands, seem to arise in unbounded quantities, and to accumulate in narrow intervals of control parameters. Numerically, we find their asymptotic rate of accumulation to be unity. The asymptotic properties of triangle vertices and their centroids are also investigated.

Introduction. – Recently, a profusion of zig-zag networks interconnecting certain classes of periodic oscillations were discovered in the control parameter space of a fiber-ring laser, in an electronic circuit containing a tunnel diode [1, 2], and in the Hénon map, a proxy for a widely used class of CO_2 lasers [3, 4]. Zig-zag networks consist of regular chains interconnecting sequences of intricate and self-similar stability phases known as *shrimps* [5]- [10], formed by pairs of cascades of either period or peak doubling bifurcations followed by chaotic oscillations. Such networks are not difficult to find in both continuous-time and discrete-time dynamical systems.

One of the distinctive characteristics of zig-zag networks is that they sometimes display infinite accumulation of shrimp triplets which form triangles, as illustrated below. Thus, they offer a natural scenario to investigate metric properties of the accumulation of bifurcation cascade whose proper unfolding requires tuning simultaneously more than one parameter. In particular, zig-zag networks allow the investigation of scaling properties of extended *areas* discovered recently in the control parameter space of prototypical systems, namely in the self-pulsations of a CO_2 laser with feedback [10, 11], in a damped-driven Duffing oscillator [12], and in the characterization of the transport properties of ratchets [13–15]. Accordingly, the present work grew out of a desire to study scaling properties of stability islands whose generic shape and position in control parameter space depend on tuning more than one control parameter simultaneously, Multiparameter scalings do not seem to have been explored yet.

As it is known, the investigation of metric properties of bifurcation cascades was the subject of several studies probing *universality classes* in dynamical systems. Such studies were motivated originally by remarkable findings reported independently by Feigenbaum [16] and by Coullet and Tresser [17, 18]. For more recent results see, e.g. Refs. [19, 20]. Despite the initial claims of universality of the scaling constants, it was concomitantly reported by several groups that the scaling constants, in fact, vary considerably in systems more complex than the quadratic map, and in higher dimensions [21]- [31].

Concerning metric properties, period-doubling bifurcations in low-dimensional systems have been studied extensively. However, such investigations were restricted exclusively to properties observed when varying a single control parameter. As it is known, the most pronounced effects of bifurcation cascades occur along certain specific directions, tortuous corridors in parameter space, which invariably require tuning more than one parameter in order to be able to move along them [5, 10]. Here, we focus on metric properties observed when complex extended structures in parameter space are deformed by the simultane-

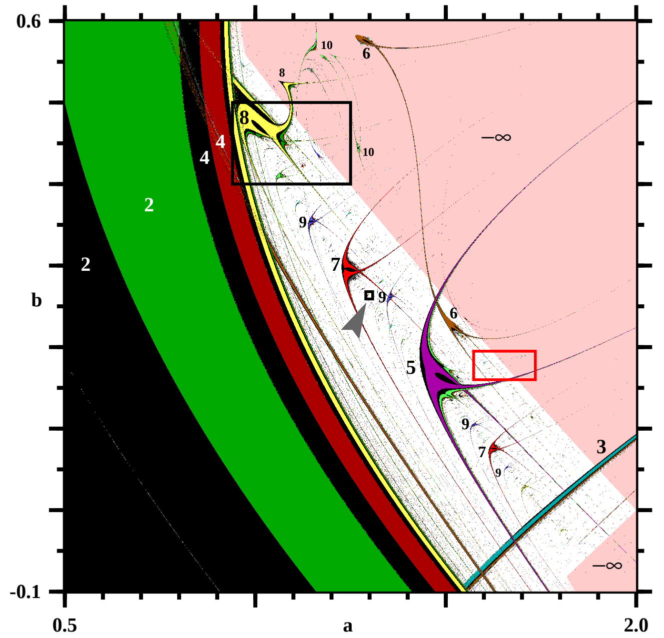

Fig. 1: The region of the control parameter space of the Hénon map which contains a large concentration of shrimplike stability structures [5]- [8]. The two colors used to display the inner structure of stability regions correspond to positive or negative values for the trace of the Jacobian matrix at every point. See Section . The arrowhead points the window magnified in Fig. 2(a). This figure displays 1200×1200 parameter points.

ous variation of two control parameters. Clearly, the need for tuning more than one parameter simultaneously arises because the boundaries separating different phases in control parameter space are normally complicated curves, not straight lines.

We report an investigation of the scaling properties of certain triangular areas delimited by shrimp triplets in the control parameter space of the two-dimensional Hénon map

$$x_{t+1} = a - x_t^2 + by_t, \qquad y_{t+1} = x_t. \tag{1}$$

Here, a, b are real parameters and x, y are real variables whose meaning depends on the particular system being modeled by the map. Figure 1 shows the distribution of stability islands for the map, with periodic phases represented in colors, following Ref. [5,10]. The triangular areas discussed here were also observed in other maps used, e.g., to model discrete ratchets, where zig-zag sequences are associated with the characterization of the ratchet current [13–15].

At present there does not exist a satisfactory and practical theory to study the accumulation of extended stability islands, that is, an analytical approach to estimate convergence of self-similar extended structures and to delimit boundaries of stability phases in higher-dimensional dynamical systems. Accordingly, such investigations must be performed numerically. For practical applications, the identification of complex structures and their accumulation mechanisms in maps can be made with a moderate investment of computer time. A significant advantage of studying metric properties of maps is the possibility to bypass all the usual uncertainties associated with numerical algorithms used for the integration of sets of differential equations.

Shrimp doublets and triplets. – Figure 1 shows a broad view of the control parameter space of the Hénon map, the region where one finds most of the shrimplike islands of stability [5]- [8]. Numbers indicate the main period k of some of the $k \times 2^n$ islands.

Rather than using eigenvalues [32], in Fig. 1 we follow Sannami [33] in plotting the *trace* τ_k of the Jacobian matrix for k-periodic points. The reason for using the trace is that eigenvalues are not always real numbers and have manifolds that may display odd behaviors [34]. Therefore, eigenvalues do not seem reliable to inspect the inner structure of shrimps. Instead of using a single solid color to paint the whole k-periodic phase, we partitioned phases into two colored sectors as follows. For a given period k, we represented the region characterized by $\tau_k > 0$ using a color associated with the period, using black to represent the region where $\tau_k < 0$. This dichotomic division of the stability windows, the same one used in all figures below, increases the information content of stability diagrams, allowing one to easily recognize shrimps sharing similar periodicities and, simultaneously, revealing their inner structure, analogously to plots of "multipliers" for one-dimensional maps [35].

In Fig. 1, the white region represents parameters leading to aperiodic (i.e., chaotic) orbits. Starting from the left side, Fig. 1 shows two pairs of stripes containing periods 2 and 4, as indicated. They belong to the familiar 1×2^n bifurcation cascade. After the rightmost period 4 region, it is possible to recognize a similar pair of parabolic stripes corresponding to period 8, also characterized by negative and positive values of τ. In the upper part of the period-8 cascade, there is a black box containing a large portion of an additional complicated period-8 structure, which extends well into the vast parameter region characterized by divergence, as indicated. This additional period-8 island contains a cusp located somewhat near structures of periods 10 and 6. Incidentally, around these islands one finds a startling phenomenon: *stable periodic orbits characterized by complex values of* (x, y) *but for real parameters* (a, b) [36].

Figure 1 also contains two boxes with shrimp doublets and triplets. As mentioned, the large and easily visible box contains part of the period 8 structure. A second and much smaller box, indicated by an arrowhead, is located between shrimps of periods 7 and 9. It is shown magnified in Fig. 2(a). At the center of this figure there is a wide period-18 stability island mentioned by Lorenz [7]. As it is clear from the figure, the trace τ reveals a relatively complicated inner topography of central portion of this island. On a finer scale, around the period 18 island there

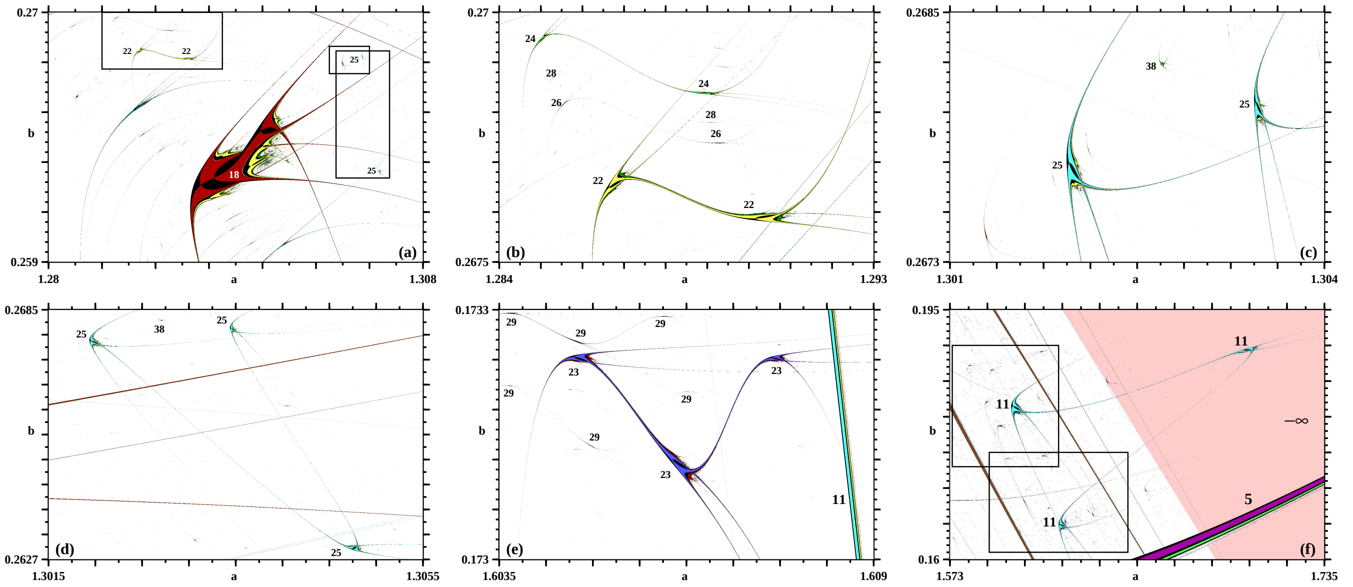

Fig. 2: Sequences of shrimp doublets and triplets. Numbers indicate the period of the main stability region. The white background represents parameters leading to chaotic oscillations. The pink background is the basin of the attractor at $-\infty$. (a) The complex period-18 structure studied by Lorenz [7], surrounded by shrimp doublets and triplets. Boxes are magnified in the next three panels. (b) A sequence of shrimp doublets. (c) An apparently isolated pair of period-25 shrimps which, however, forms (d) A shrimp triplet. (e) A period-23 triplet between a pair of period-29 triplets. (f) A region with a profusion of triplets and more intricate stability islands. The two boxes are magnified in Fig. 6. Individual panels display the analysis of $1200 \times 1200 = 1.44 \times 10^6$ parameter points.

is a profusion of shrimp doublets, some of which are shown in Fig. 2(b). Sometimes, such doublets are in fact triplets, which may also arise as combinations of unsuspected and apparently uncorrelated structures, as shown in Fig. 2(c) and Fig. 2(d).

As hinted by the periodicities of individual doublets in Fig. 2(b), they do not seem to be connected in any noticeable way. Uncorrelated doublets exist also in several other locations in the control parameter plane. Analogously, there is a large number of triplets, like in Fig. 2(d), which do not seem to be connected to other stability islands. Attempts to detect shrimp connections met difficulties because their legs get thinner and thinner as one moves away from their central stability region. Similarly to Fig. 2(d), Figure 2(e) illustrates a period-23 triplet formation in the same parameter region where there are two period-29 triplets. Such mixed formations are also found in other windows in the $b > 0$ half of the control plane. Figure 2(f) shows a sort of "border line" triplet straddling the chaotic and the divergent backgrounds, namely a triplet having two shrimps located over a background of chaos linked to a shrimp located over the background of divergence. Near this triplet, one finds a plethora of additional triplets as well as more complicated arrangements, illustrated by the pair of boxes in Fig. 2(f), shown magnified below in Fig. 6. In contrast to the isolated doublets and triplets in Fig. 2, it is also possible to find unbounded cascades of self-similar triplets forming *arithmetic progressions*, namely whose periodicity increases by a constant value from triplet to triplet, as illustrated in Fig. 5 and discussed in the next Section.

Triplets in arithmetic progression. – Figure 3 shows a sequence of successively magnified windows indicating the location of an interesting arithmetic progression of shrimp triplets that we wish to consider in more detail. The pair of boxes Fig. 3(a) contains several triplets analogous to the ones observed in systems governed by differential equations, namely in fiber-ring lasers, and in an electronic circuit with a tunnel diode [1,2]. Figure 3(b) shows uncorrelated triplets similar to the ones in Fig. 2(d), while the red boxes in Figs. 3(c) and 3(d) mark the location of triplets in an apparently never-ending arithmetic progression. Similar unbounded progressions exist in other parameter windows, particularly for orbits of higher periods. Such apparently unbounded progressions of stability islands display accumulation boundaries, horizons, embedded in the broad parameter background associated with chaotic oscillations.

The study of metric properties of the two-dimensional Hénon map and higher dimensional maps is more complicated than the corresponding study for one-dimensional systems. For one-dimensional maps $x_{i+1} = f(x_i)$, the study of metric properties is greatly facilitated by the presence of *critical points*, namely points where $df(x)/dx|_{x=x_i} = 0$. Orbits containing such points are the so-called *superstable orbits*. For such orbits, the *multiplier* $m_k \equiv df_k/dx$ associated with a k-periodic orbit is

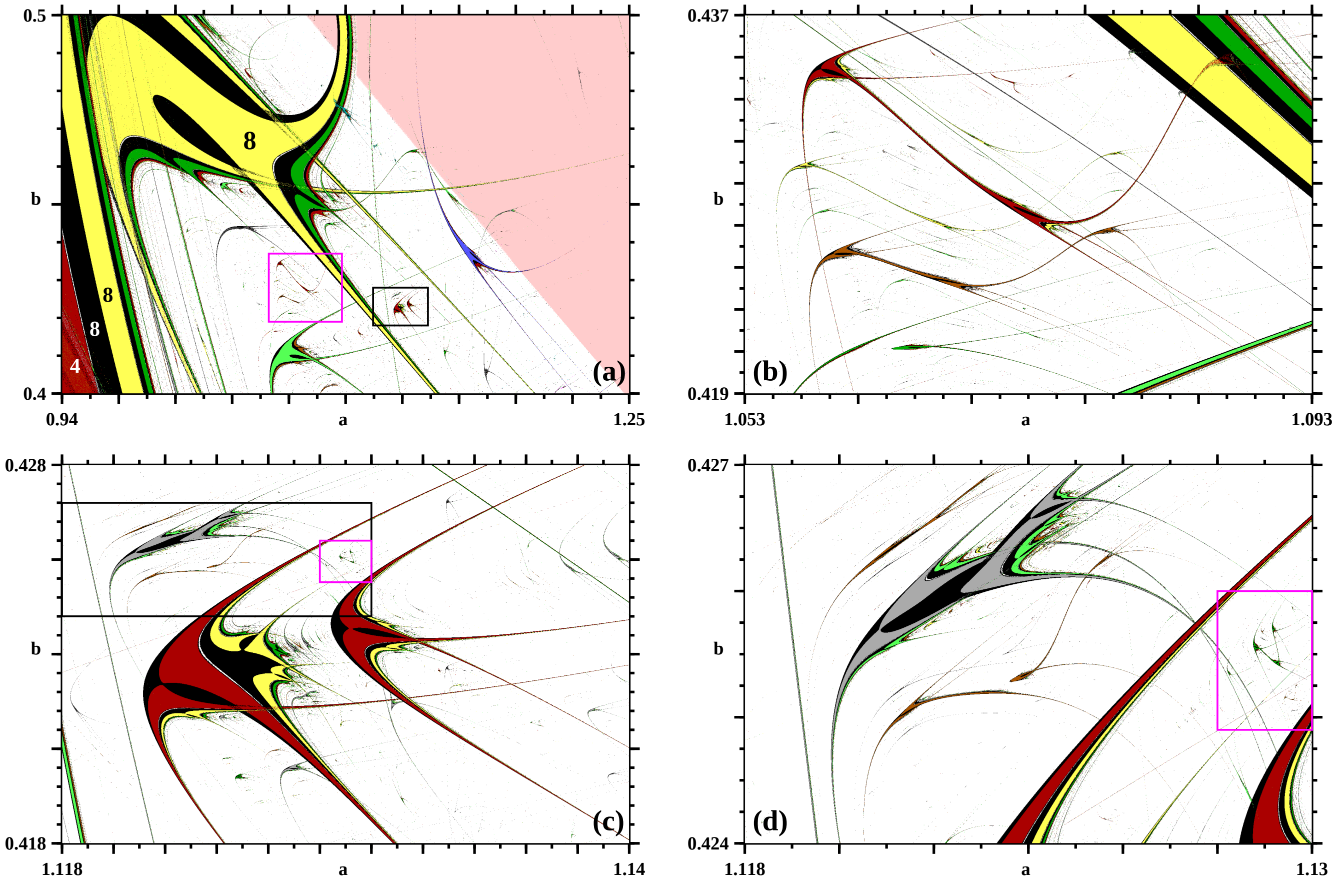

Fig. 3: Successive magnifications illustrating a profusion of zig-zag triplets. (a) Magnification of the uppermost box in Fig. 1. (b) Enlargement of the red box in (a). (c) Enlargement of the black box in (a). (d) Apparently unbounded arithmetic progression of zig-zag triplets is located in the box, shown magnified in Fig. 5. Similar sequences exist in other regions of the control parameter space. Grid resolution: 1200 × 1200 parameter points.

zero [37–39] (f_k denotes the k-th composition of f with itself) [35]. Critical points are the basic objects used by Fatou and Julia to study the properties of iterated rational functions. For a very complete survey of the classical literature see Cremer [39]. For more recent literature consult Ref. [40]. Unfortunately, for high-dimensional maps there are no proper definitions for critical points, multipliers, and superstable orbits.

Figure 4 shows enlarged views of the three shrimps forming the vertices $A_1B_1C_1$ and $A_2B_2C_2$ of first two triplets in arithmetic progression. From Fig. 4 one clearly sees that the trace of the Jacobian matrix is not equivalent to the multiplier. For, although the trace is capable of exposing two parabolic arcs which resemble the parabolas generated by multipliers for one-dimensional maps, for the Hénon map the parabolic arcs are "broken", i.e., they do not always intersect, as in panels A_1, B_1, A_2, B_2, C_2. Furthermore, when they do intersect, the intersection occurs is not at just a single point but, instead, in an extended region, as seen in panel C_1. These two problems are generic difficulties present in all higher dimensional systems. To bypass trace peculiarities and to be able to define unambiguously all shrimp *heads* [35], here we interpolated broken parabolic arcs and used their points of intersection to define triangle vertices.

Areal scaling. – Figure 5 shows the location and the strong compression undergone by the first 11 triangle triplets which accumulate in arithmetic progression towards the period-18 boundary as they successively get more and more squeezed. Red dots mark the centroid of the triangles, namely the intersection of the three triangle medians. The coordinates of the triangle vertices are recorded, their area, and their centroid coordinates are collected in Table 1. These numerical values were obtained by measuring them from individual blowups (not given here) for every triangle. Noteworthy is the fact that the period difference between two consecutive triangles is 18, the same period boundary horizon towards which they accumulate. As mentioned above, this situation is analogous to the one previously observed in a damped-driven Duffing oscillator [12] and in the self-pulsations of a CO_2 laser with feedback [10, 11].

As seen from Fig 5, vertices tend to accumulate fast, in a narrow parameter interval. This tendency may also

Table 1: Period k_i, coordinates, areas and centroids of the triangles in arithmetic progression, shown in Fig. 5. The values in the bottom line are extrapolated values. See text.

i	k_i	a_{A_i}	b_{A_i}	a_{B_i}	b_{B_i}	a_{C_i}	b_{C_i}	Area $\times$ 10^8	a_{centroid}	b_{centroid}
1	44	1.12878432	0.42556190	1.12924456	0.42542796	1.12917220	0.42570713	5.93966512	1.12906703	0.42556566
2	62	1.12942445	0.42515476	1.12958722	0.42513889	1.12966421	0.42525273	0.98757841	1.12955863	0.42518213
3	80	1.12957064	0.42504772	1.12967360	0.42505563	1.12976177	0.42513312	0.36404728	1.12966867	0.42507882
4	98	1.12962318	0.42500862	1.12970509	0.42502402	1.12979458	0.42508885	0.19660397	1.12970762	0.42504050
5	116	1.12964741	0.42499058	1.12971932	0.42500938	1.12980916	0.42506822	0.12710962	1.12972530	0.42502273
6	134	1.12966058	0.42498084	1.12972700	0.42500162	1.12981689	0.42505705	0.09068732	1.12973482	0.42501317
7	152	1.12966845	0.42497497	1.12973143	0.42499706	1.12982147	0.42505030	0.06820358	1.12974045	0.42500744
8	170	1.12967360	0.42497118	1.12973422	0.42499418	1.12982446	0.42504592	0.05295770	1.12974409	0.42500375
9	188	1.12967713	0.42496855	1.12973609	0.42499224	1.12982644	0.42504289	0.04229662	1.12974655	0.42500123
10	206	1.12967971	0.42496670	1.12973741	0.42499088	1.12982789	0.42504073	0.03442693	1.12974834	0.42499944
11	224	1.12968156	0.42496529	1.12973837	0.42498989	1.12982896	0.42503912	0.02841212	1.12974963	0.42499810
⋮	⋮	⋮	⋮	⋮	⋮	⋮	⋮	⋮	⋮	⋮
55	1016	1.12968365	0.42496342	1.12973944	0.42498857	1.12982988	0.42503696	0.02129941	1.12975092	0.42499632

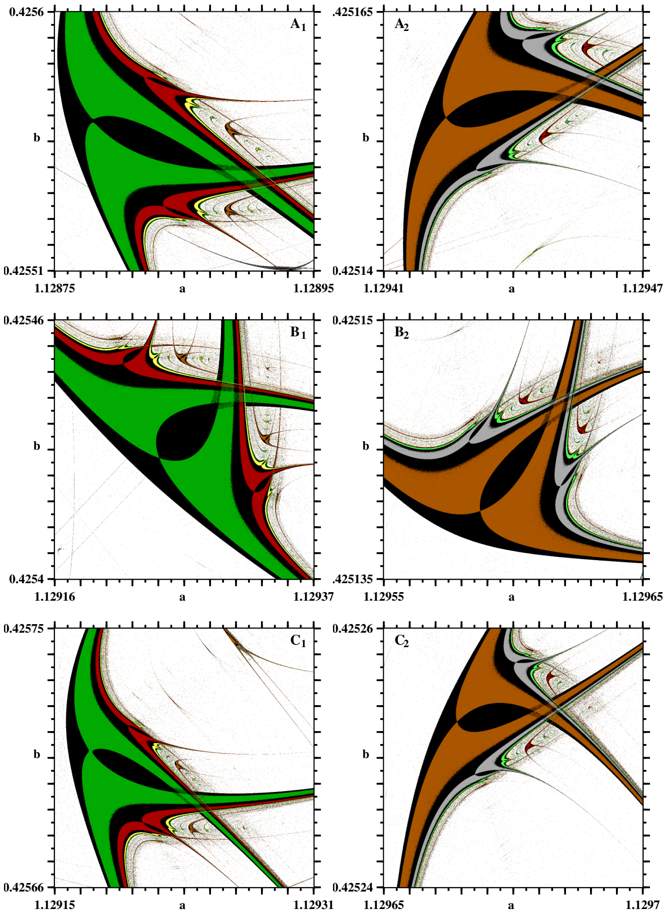

Fig. 4: Details of the arithmetic progression of triplets accumulating towards the period-18 domain. Left column: triplet A_1, B_1, C_1, each of main periodicity 44. Right column: triplet A_2, B_2, C_2 of main periodicity 62. An apparently unbounded quantity of additional triplets exist. Note that the parabolic arcs defining shrimp “heads” [35] may meet or not (see text). Individual panels displays $1200 \times 1200 = 1.44 \times 10^6$ parameter points.

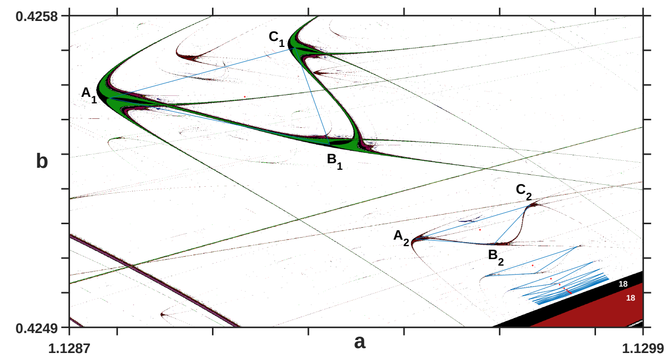

Fig. 5: The first 11 triangles of an apparently infinite arithmetic progression accumulating towards a period-18 boundary. The difference of the periods between two consecutive triangles is also 18. Grid resolution: 3000×3000 parameter points.

be seen in Table 1. Accordingly, an interesting issue is to determine their accumulation points and rate of convergence. To find them, we proceed as follows: (i) Firstly, we compute the successive differences between the coordinates (a, b) for vertices and centroids of each triangular region; (ii) From these differences, a fitting equation for each sequence is derived; (iii) Using these fitting equations we estimate the coordinates for extrapolated triangles; (iv) The extrapolation process is extended until quantities remain constant to eight decimal digits. The convergence rate of the triangles towards the asymptotic horizon is found to be unity. The resulting extrapolated values are listed in the last line of both tables above. For $i = 55$, the listed values for the area and centroid were obtained from the extrapolation, not from the vertices coordinates in the table, although both sets of values essentially coincide. Remarkably, triangles seem to accumulate just before reaching the period-18 horizon leg in front of them. Perhaps extrapolations using more than 11 triangles could reveal the extrapolated values come closer or even coincide asymptotically with the convergence horizon. However, it becomes increasingly more difficult to reliably detect triangles when the period further increases. The precise location of the convergence horizon is therefore left as an open question for further investigation.

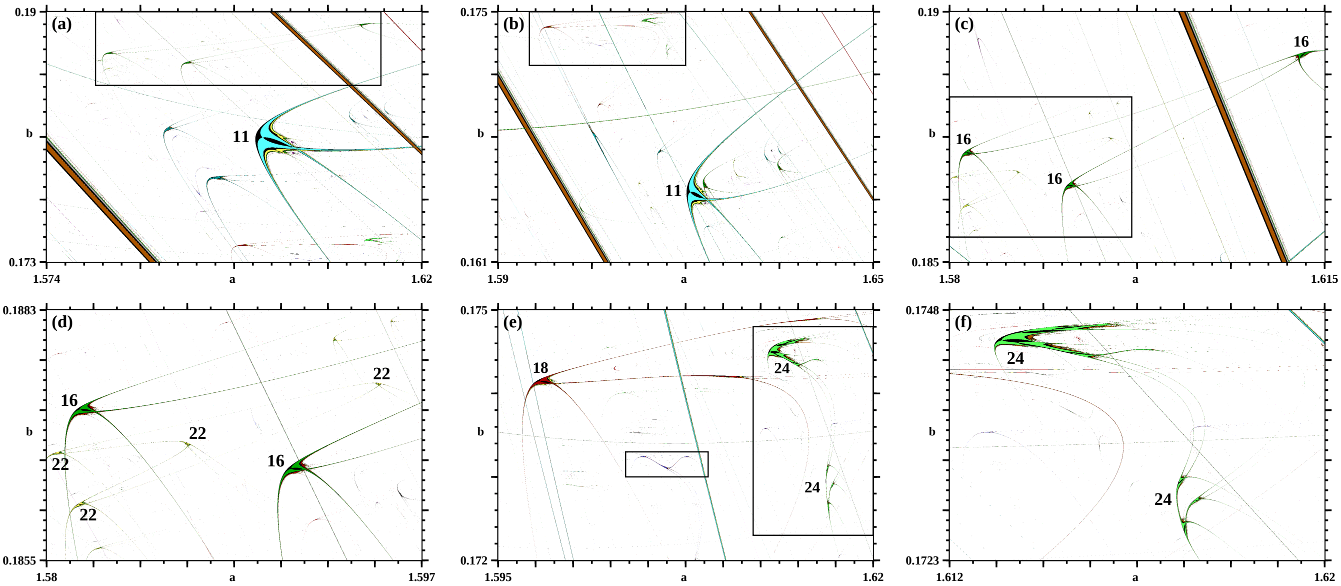

Fig. 6: Magnifications of the pair of boxes seen in Fig. 2(f) showing some exquisite and much more complicated triplets.

As a last result, in Fig. 6 we collect a number of triangular stability islands which "break the symmetry," namely that do not fit unambiguously in the above scenarios but, instead, display more exquisite shapes and organizations. For instance, the box in Fig. 6(a), magnified in Fig. 6(c), displays a pair of shrimps that under low resolution may appear as uncorrelated but that are in fact interconnected, forming a triplet. Figure 6(d) shows that a period-22 triplet is partially overlapping the leftmost partner of a larger period-16 triplet. In reality, the period-22 triplet is interconnected with a fourth shrimp locate farther to the right, as indicated. Therefore, it is possible to circulate continuously from one shrimp to the others without ever having to cross the vast sea of chaos surrounding them. Several additional triplets exist in these regions, but are too small to be identified under low resolution. Analogously, Fig. 6(b) contains several triplets that may be easily seen under higher resolution. Of particular interest in this panel is the region inside the box, magnified in Fig. 6(e). First, the leftmost and smaller box shows a sort of symmetric triplet which also exists in other regions of the parameter space. However, the most curious triplet is located inside the rightmost box, magnified in Fig. 6(f). In this box, one finds a period-24 triplet that is interconnected with a very complex structure of the same period. Such highly complex structures exist abundantly and are frequently found to be interconnected with less complicated structures sharing the same period. As is known, at present there is no theoretical framework to explain the origin of any of such structures, highly complex or not.

Conclusions and outlook. – We studied metric properties of certain triangular stability islands covering extended areas in control parameter space and which are abundantly present in flows and maps. Such triangular islands appear both isolated form or forming apparently unbounded arithmetic progressions. In contrast with the familiar scalings in the literature, the unfolding of areal scaling requires tuning more than one control parameter simultaneously. A significant feature of the arithmetic progression is that it displays specific accumulation points, both for triangle vertices and their centroid coordinates. Although the emphasis here was on a specific period-18 accumulation, we find accumulations to be a rather common phenomenon, involving analogous arithmetic progressions and many other periods. The accumulation unfolds systematically and is fast. Accordingly, the convergence to an almost constant value of the area was observed. Furthermore, we find the arithmetic progression to converge to a well-defined asymptotic horizon whose period coincides with the constant rate of period increase of the arithmetic progression. It is not yet clear if the arithmetic progressions involve a finite or an infinite number of terms. A particularly promising system for investigating two-parameter scalings is the analytical path discussed in Fig. 2 of Ref. [41], for the so-called *canonical quartic map*. In conclusion, the metric properties of extended progressions of stability structures whose accumulation in control parameter space depends on more than one parameter were studied in detail and characterized numerically. We are not aware of any previous study of the scaling of properties depending on the variation of more than one parameter simultaneously. Our results are also relevant for flows, systems governed by differential equations. It would be interesting to compare the present findings with analogous ones for ratchets and the aforementioned flows representing semiconductor laser diodes, electronic circuits, and other promising systems.

* * *

This work was supported by the Max-Planck Institute for the Physics of Complex Systems, Dresden, in the framework of the *Advanced Study Group*: *Forecasting with Lyapunov vectors*. IMJ was supported by the Hungarian National Research, Development and Innovation Office under grant K-125171. JACG was also supported by CNPq, Brazil.

REFERENCES

[1] Francke R.E., Pöschel T. and Gallas J.A.C., Phys. Rev. E **87** (2013) 042907.
[2] Francke R.E., Pöschel T. and Gallas J.A.C., Infinite networks of hubs and spirals in an erbium-doped fiber-ring laser, in *Advances in Nonlinear Dynamics Synchronization with Selected Applications in Theoretical Electrical Engineering*, Chapter 10, Edited by K. Kyamakya, W.A. Halang, W. Mathis, J.C. Chedjou, and Z. Li (Springer Verlag, Berlin, 2013).
[3] Bonatto C., Garreau J.C. and Gallas J.A.C., Phys. Rev. Lett. **95** (2005) 143905.
[4] Bonatto C. and Gallas J.A.C., Phys. Rev. Lett. **101** (2008) 054101. Phil. Trans. Royal Soc. London, Series A **366** (2008) 505-517.
[5] Gallas J.A.C., Phys. Rev. Lett. **70** (1993) 2714-2717.
[6] Hunt B.R., Gallas J.A.C., Grebogi C., Yorke J.A. and Koçak H., Physica D **129** (1999) 35-56.
[7] Lorenz E.N., Physica D **237** (2008) 1689-1704.
[8] Façanha W., Olderman B. and Glass L., Phys. Lett. A **377** (2013) 1264-1268.
[9] Maranhão D.M., Phys. Lett. A **380** (2016) 3238-3243.
[10] Gallas J.A.C., Adv. Atom. Molec. Opt. Phys. **65** (2016) 127-191.
[11] Junges L. and Gallas J.A.C., Opt. Commun. **285** (2012) 4500-4506.
[12] Bonatto C., Gallas J.A.C. and Ueda Y., Phys. Rev. E **77** (2008) 026217.
[13] Celestino A., Manchein C., Albuquerque H.A. and Beims M.W., Phys. Rev. Lett. **106** (2011) 234101.
[14] Manchein C., Celestino A. and Beims M.W., Phys. Rev. Lett. **110** (2013) 114102.
[15] Carlo G.G., Ermann L., Rivas A.M.F. and Spina M.E., Phys. Rev. E **99** (2019) 012214.
[16] Feigenbaum M., Los Alamos Science, Summer 1980, pages 4-27.
[17] Coullet P. and Tresser C., J. Phys. Colloq. **C5-39** (1978) C5-25–C5-28.
[18] Coullet P., Tresser C. and Arneodo A., Phys. Lett. A, **72** (1979) 268-270.
[19] Lyubich M., Ann. Math. **149** (1999) 319-420.
[20] Tresser C., Coullet P. and de Faria E., Period doubling, Scholarpedia **9** (2014) 3958. `http://www.scholarpedia.org/article/Period_doubling`
[21] Derrida B., Gervois A. and Pomeau Y., J. Phys. A **12** (1979) 269-296.
[22] Benettin G., Cergignani C., Galgani L. and Giorgilli A., Lett. Nuovo Cimento **28** (1980) 1-4.
[23] Benettin G., Galgani L. and Giorgilli A., Lett. Nuovo Cimento **29** (1980) 163-166.
[24] Derrida B. and Pomeau Y., Phys. Lett. A **80** (1980) 217-219.
[25] Collet P., Eckmann J.P. and Lanford O.E., Commun. Math. Phys. **76** (1980) 211-254.
[26] Green J.M., MacKay R.S., Vivaldi F. and Feigenbaum M., Physica D **3** (1981) 468-486.
[27] Bountis T.C., Physica D **3** (1981) 577-589.
[28] Coste J. and Peyraud N., Physica D **5** (1982) 415-420.
[29] Ostlund S., Rand D., Sethna J. and Siggia E., Physica D **8** (1983) 303-342.
[30] Eckmann J.P. and Wittwer P., J. Stat. Phys. **46** (1987) 455-475.
[31] Kusnetsov S.P., Mailybaev A.A. and Sataev I.R., J. Stat. Phys. **130** (2008) 599-616.
[32] Hitzl D.L. and Zele F., Physica D **4** (1985) 305-326.
[33] Sannami A., Japan J. Appl. Math. **6** (1989) 291-330.
[34] Beims M.W. and Gallas J.A.C., Scientific Rep. **6** (2016) 18859.
[35] Gallas J.A.C., Physica A **202** (1994) 196-223.
[36] Endler A. and Gallas J.A.C., Comptes Rendus Mathem. (Paris) **342** (2006) 681-684.
[37] Schröder E., Math. Ann. **2** (1870) 317-365.
[38] Böttcher L.E., Izv. Kazan Fiz.-Mat. Obshch. **14** (1904) 155-234.
[39] Cremer H., Jahresber. Deutsche Math. Ver. **33** (1925) 185-210.
[40] Alexander D.S., Iavernaro F. and Rosa A., Early days in complex dynamics: a history of complex dynamics in one variable during 1906-1942 (American Mathematical Society, Providence, 2012).
[41] Gallas J.A.C., Physica Scripta **94** (2019) 014003, Festschrift Wolfgang Schleich.